

Multiphase flow metering for the oil and gas industry using a visualisation technique

Syed F. A. Bukhari, Francesco Coletti, Carola S. König, Tassos G. Karayiannis

Abstract—Measuring multiphase flows accurately and reliably, particularly when three or more phases are involved, is a challenging and long-standing problem in the upstream oil-and-gas industry. Crude oil extracted from the reservoir is a complex mixture that contains oil, water, gas and sand. Before it is further transported downstream, the crude oil is typically processed in a pressure vessel that separates oil, water and gas. To reduce costs and increase safety, it is critical to accurately measure the streams flow rate (two- and three-phase) at this stage. The conventional metering systems require test separators, where the flow is diverted and measured. This method requires additional capital equipment, large maintenance cost and constant operator intervention. In this paper, a non-intrusive technology that continuously measures multi-phase flow is proposed to overcome the limitations of traditional systems. The novel multiphase flow metering system is based on the combined use of electrical capacitance tomography (ECT) images and knowledge base which is envisaged to provide continuous accurate, reliable, non-intrusive measurements at a minimal cost. In this technique, two ECT sensors are placed at two different locations in an oil pipeline. A hybrid technique is used to evaluate ECT images based on principal component analysis (PCA) and cluster analysis (CA) to identify the time interval, when a specific process condition is detected in both sensors. Once this information is obtained, volumetric flow rate and mass flow rate can then be calculated using the cross sectional area of the pipeline and the average velocity. Initial results with imaging sensors at two points indicate that an error of less than 5% can be achieved, which is acceptable for most applications in the oil and gas industry. This measurement method can be further extended by using three or more points for increased reliability and accuracy.

Keywords— cross correlation, flow meter, multiphase flow, oil-and-gas, visualisation technique.

I. INTRODUCTION

In many industries, particularly in oil and gas, measuring accurately and reliably multiphase flows is of paramount importance. The traditional flow include high cost, inaccuracies especially for multiphase flows, insensitivity to small changes and provide no insight about the process on the contrary visualisation techniques have the advantage that they are accurate, have high sensitivity and can provide visual knowledge of the process condition.. Therefore by using visualisation technique timely corrective actions can be taken to avoid any undesirable situation in the process, e.g. blockage in oil pipe line. In recent years, extensive research has focused

on measurement and control of different industrial processes using various visualisation techniques, such as electrical capacitance tomography (ECT), electrical resistance tomography (ERT) and high-speed, high-resolution cameras [1]-[3]. These techniques have successfully been used to visualise flow in oil separators and fluidized beds in the past [15]-[16]. Based on initial results, this visualising technique provides promising method than conventional techniques for multiphase flow metering.

Research using ECT for example is in progress at the University of Manchester [4]. Flow visualisation systems based on ECT are available commercially [5]. However, traditional applications focus on treating water and oil as two separate continuous liquid phases using one ECT sensor. As a result, the velocity profile of the flow cannot be estimated. In this paper, we propose the use of a novel approach to multi-phase flow metering that entails the use of two or more ECT sensors placed at different points in the pipeline. This approach, combined with statistical techniques and a knowledge base system will allow calculating the velocity profile inside a pipeline transporting oil and gas flows.

A. Challenges Associated with Visualisation Techniques

For visualisation techniques to be effectively applied to multiphase flow metering, the overall device should be accurate, relatively inexpensive and inherently insensitive to the variations in flow regime. Table 1.1 summarises different features of the various techniques available.

While flow visualisation techniques have distinct benefits for example the flow regime can be determined in order to compensate the non-linearity of currently available MPF meter, however, there are some challenges associated with these techniques. The most important one is the development of accurate mathematical model that enable an accurate estimation of volume flows. A related challenge is the computational time needed to solve such models. This is because accurate image reconstruction and image processing for knowledge base are both computation intensive. Another practical aspect is the mechanical and electronic hardware design for safe and reliable use in the harsh environment typical of the oil and gas industry.

S. F. A. Bukhari is with the College of Engineering, Design and Physical Sciences, Brunel University London, Uxbridge, UB8 3PH, UK (corresponding author, phone: +44-7715-640-687; e-mail: syed.bukhari@brunel.ac.uk).

F. Coletti is with the College of Engineering, Design and Physical Sciences, Brunel University London, Uxbridge, UB8 3PH, UK (e-mail: francesco.coletti@brunel.ac.uk).

C. S. König is with the College of Engineering, Design and Physical Sciences, Brunel University London, Uxbridge, UB8 3PH, UK (e-mail: carola.koenig@brunel.ac.uk).

T. G. Karayiannis is with the College of Engineering, Design and Physical Sciences, Brunel University London, Uxbridge, UB8 3PH, UK (e-mail: tassos.karayiannis@brunel.ac.uk).

TABLE I
COMPARISON OF VISUALISATION TECHNIQUES

Measurement method	Accuracy	Substances	Limitations	Cost
<u>Tomography based techniques:</u>				
Gamma-ray and X-ray transmission tomography	0.05 %	Gas/liquid pipe flow	Scanning time longer, images not sharp	High
Electrical capacitance tomography	±2-3%	Gas, water, oil and solid flows	Online calibration is difficult	High
Microwave tomography	1.4-13.1%	Gas and oil multiphase flow	Quantitative imaging not possible	Low
<u>Optical particle tracking methods:</u>				
Cinematography	2%	Air-solid particle flow	Slow shutter speed produces error	High
Laser Doppler anemometry	-0.16-0.84%	Air, water flow	Not suitable for cross correlation	Med. to High
Particle image velocimetry	3.1%	Swirling flow	Limited temporal resolution	Med. to High

B. Tomography Based Visualisation Techniques

Tomography is a combination of two words “tomo” means a cutting or a section and “graphy” means photo. Tomography is a visualisation technique, which is non-invasive and non-intrusive. This technique has been effectively used to provide concentration, holdup or the spatial density distributions of at least one component of any multiphase system. The tomography and radiography systems can be categorised mainly in the following three categories [6]-[7]:

(1) Nuclear based imaging techniques using ionising radiations:

- Gamma-ray and x-ray transmission tomography
- Positron emission tomography
- X-ray diffraction micro-tomography
- X-ray and neutron transmission radiography

(2) Nuclear-based but non-ionising imaging techniques:

- Nuclear magnetic resonance (NMR) imaging

(3) Non-nuclear based imaging techniques:

- Electrical capacitance tomography (ECT)
- Optical tomography
- Ultrasound tomography
- Microwave tomography

Of the techniques above, only gamma-ray and x-ray transmission tomography, microwave tomography and ECT have been used in multiphase flow measurements. In gamma ray and x-ray transmission tomography, the attenuation of a beam of gamma-rays or x-rays is measured after it has passed through a heterogeneous medium. This is done with different orientation of the volume under investigation. After taking measurements, an image of the process is reconstructed that gives density distribution of different materials. Since the data collection and image reconstruction are performed by computer therefore this technique is known as computer-assisted tomography (CAT) or computed tomography (CT). This technique has been applied to identify the flow regime of gas/liquid flows. Different features, such as spatial resolution, response time and the measurement resolution of the attenuation coefficient are used to monitor the performance of these systems (Maad and Johansen 2008). However, it has the disadvantage that the measurement geometry and the reconstruction method can affect the error of the reconstructed pixel values.

Microwave tomography (MWT) is a non-ionizing technique. This technique is used to extract the dielectric profile of an object in the form of a quantitative image using data collection/calibration and data processing. Data collection is done firstly in the absence of the object of interest known as incident-field data set and secondly in the presence of the object of interest known as total-field data set. Then the scattered field data set is obtained by subtracting the incident-field data set from the total-field data set. This measured scattered field data set is then calibrated for use in data processing to get the quantitative image of the process. Like ECT, appropriate inversion algorithms mostly nonlinear are used for image reconstruction in microwave tomography [9].

ECT provides a non-invasive and non-intrusive method (as mentioned previously) to obtain cross sectional images of the interior of the process vessels, which can be used to monitor and control the process operations. This can also be used as a model validation tool in process design [10]-[11]. ECT has been successfully used for processes involving non-conducting materials of different permittivity or mixtures [12].

In this research, ECT sensors are used for developing a novel method for measuring multiphase flow in oil pipelines.

II. OVERVIEW OF ECT

ECT is a soft-field tomography therefore it requires complex image reconstruction. There is a non-linear relationship between the measurements and the permittivity distribution. If free electrical charge is not enclosed in the electrical field inside the measurement plane then the relationship between capacitance and permittivity distribution is governed by [13]:

$$\nabla \cdot [\varepsilon(x, y) \nabla \phi(x, y)] = 0 \quad (1)$$

$$C = \frac{Q}{V} = -\frac{1}{V} \iint_{\Gamma} \varepsilon(x, y) \nabla \phi(x, y) d\Gamma \quad (2)$$

where ∇ is the gradient operator, $\varepsilon(x, y)$ is the permittivity distribution in the sensing field, $\phi(x, y)$ is the electrical potential distribution, V is the potential difference between two electrodes forming the capacitance and Γ is the electrode surface. The boundary conditions when one electrode is excited with a fixed voltage V_o and all other electrodes are kept at zero potential, as occurs during the measurement procedure, are defined by

$$\begin{aligned} \phi &= V_o \quad (\text{for the excited electrode}) \\ \text{and } \phi &= 0 \quad (\text{for others}) \end{aligned} \quad (3)$$

A. ECT Sensor

There are two important steps for information retrieval in ECT, i.e. capacitance measurements and image reconstruction. In ECT, the measurement procedure is simple because each electrode is energised by applying an excitation voltage and the induced charge is detected from all other electrodes, while their electric potential is kept at zero. For example, in an 8-electrode ECT sensor (Fig 1) electrode 1 is used as the excitation electrode and electrodes 2 to 8 as detection electrodes. In the next step electrode 2 is used as the excitation electrode and electrode 3 to 8 as the detection electrodes and so on. This is repeated until electrode 7 is used as the excitation electrode and electrode 8 as the detection electrode. In this way, for an ECT sensor with N electrodes, $N(N-1)/2$ independent capacitance measurements are taken. Although construction of an ordinary ECT sensor is relatively easy but when sensitivity is required for getting optimal performance, this step becomes extremely complex.

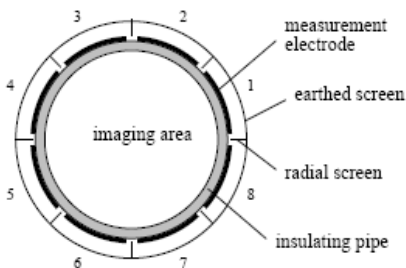


Fig 1 ECT sensor with 8 electrodes

B. Image Reconstruction Algorithms for ECT

For ECT image reconstruction a number of algorithms are available, such as linear back projection (LBP), singular value decomposition (SVD), Tikhonov regularisation, Newton-Raphson, steepest descent method, Landweber iteration, conjugate gradient method, algebraic reconstruction technique (ART), simultaneous iterative reconstruction technique (SIRT) and model-based reconstruction [14]. The selection of a reconstruction algorithm depends on desired speed and accuracy. Iterative algorithms can increase the accuracy, but

they reduce the speed. For fast on-line imaging, the LBP algorithm is probably the best if only a reasonable accuracy is required. When high accuracy is desirable more complicated algorithms are preferred. Iterative image reconstruction is time-consuming, because the estimation of capacitance from an image usually involves finite element analysis. Because of the faster processing need, LBP is used in this work.

C. ECT Sensor Calibrations

Normally an ECT sensor is calibrated using two materials of high and low permittivity to define the limits. With a three phase mixture of air, oil and water, the air and oil components cannot be resolved if normal calibration method is applied. In this work, a different approach will be used for visualisation by incorporating more than two materials for calibration. This is because the relative permittivity values of air and oil are close, i.e. 1 and 2.1 respectively compared to water at about 80. To image air, oil and water, an ECT sensor is calibrated by air, oil and water instead of air and water only. When a set of capacitance readings has been acquired from an ECT sensor, one image is generated using the air-oil calibration data to reflect the contrast between air as one component and oil and water as another component. A second image is then generated using the air-water calibration data to reflect the contrast between air and oil as one component and water as another component. Then image fusion is applied to combine the two images together to illustrate three-component distribution. Images for different air, oil and water levels are shown below in Fig 2. Many such images are generated to construct a knowledge-base, which is being used for generating control signals.

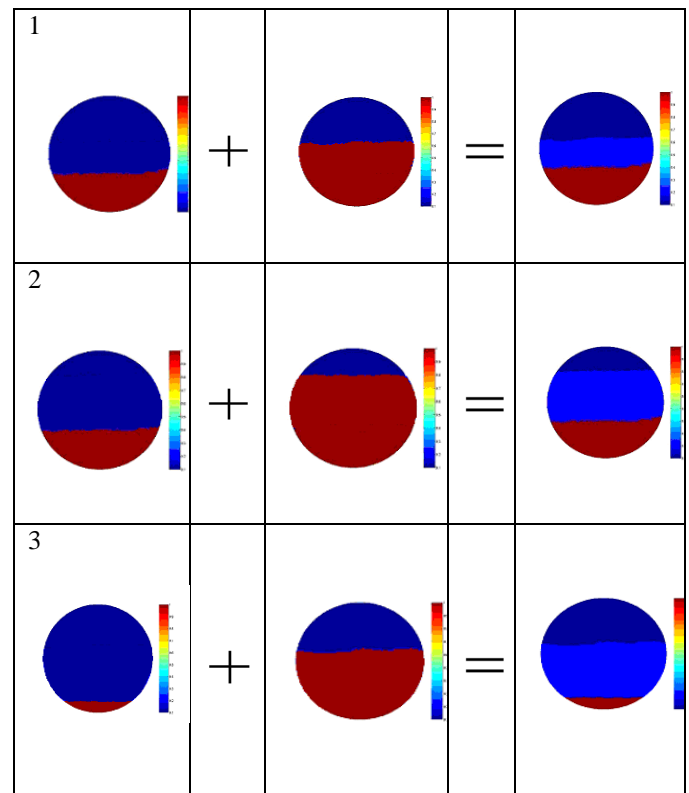


Fig 2 Process images for different conditions

III. MULTI-ECT SENSORS BASED MPF METER

A new concept of MPF meter is presented in this paper using ECT technique (Fig 1) that can provide image of the complete process flow. This type of meter is conceptually simple and inherently insensitive, unlike commercially available visual flow meters, to the variations in flow regime. Another advantage of using visualisation technique as a tool is to determine the flow regime in order to compensate the non-linearity of currently available MPF meters. This MPF meter can provide images of the process from two points instead of one so that velocity profile could be calculated using cross correlation technique. It is also expected that it will address inaccuracies in volume flow estimations by the use of more accurate model. In order to get readings from 0 to 100% range, a hybrid technique based on principal component analysis (PCA) and cluster analysis (CA) is used. PCA is used because it is a dimension-reduction tool that can be used to reduce a large set of variables to a small set that still contains most of the information in the large set. On the other hand CA is used for the task of grouping a set of objects in such a way that objects in the same group are more similar to each other than to those in other groups. This will help in obtaining estimations even in a condition that is unpredictable. Since for CA to work, it is not necessary to match data exactly rather information are classified on the basis of the closed match. In this research, however, there is still be a need for high-performance computing (accurate image reconstruction and the subsequent cross-correlation process are both computation-intensive) for improved data processing efficiency. Fig 3 shows a conceptual diagram of this proposed flow meter.

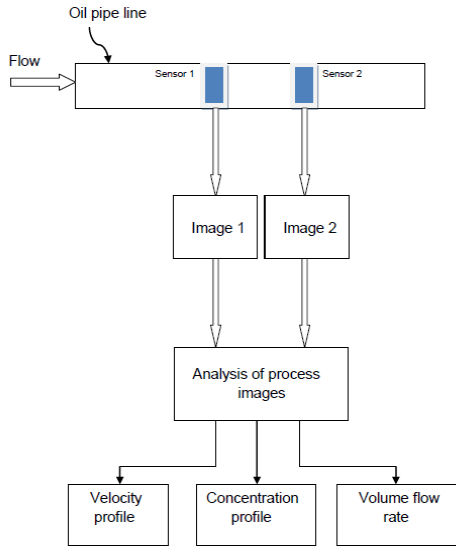


Fig 3 Visualisation technique for MPFM in oil pipe line

In this work, the images are obtained using two high resolution ECT sensors (Fig 3) because the performance of any MPF system certainly depends on the measurement accuracy of the process parameters [1]. After image analysis (Section 2.3), a hybrid technique is applied on the process images to find the closest condition in the knowledge base.

A. Knowledge based Hybrid Monitoring Strategy

In this work, PCA has been used for generating precise prior information using a model-based approach. Then cluster analysis is used to see the closest stored condition to the current situation, i.e. the measured image, thus taking advantages of both techniques. This technique starts by capturing the raw data from the ECT system and ends with the generation of a control signal required. The first step, i.e. filtering is used for the generation of data for the knowledge base. After filtering of data, the principal component analysis part starts.

PCA is used for segmentation and image interpretation. The basis for these steps is to evaluate only those components needed for decision-making. It has an advantage of having only essential information and avoids storing information of every pixel. The segmentation starts from reading an ECT image. In this step, the threshold is used to convert values of pixels to three colours (dark blue, blue and red representing air, oil and water respective, see Fig 2).

$$V_{DB} = \text{Range of threshold for dark blue} \quad (4)$$

$$= 112 \leq V_{DB} \leq 128$$

$$V_B = \text{Range of threshold for blue} \quad (5)$$

$$= 129 \leq V_B \leq 140$$

$$V_R = \text{Range of threshold for red} \quad (6)$$

$$= 141 \leq V_R \leq 255$$

By using above threshold values, ECT images with different pixel values are converted to only dark blue, blue and red colours. After image segmentation, the next step will be to count number of different colour pixels (Image interpretation). If N_{DB} , N_B and N_R represent number of pixels of dark blue, blue and red pixels respectively and N_T is the total number of pixels in the image then the percentages of air, oil and water can be calculated as

$$\text{Water percentage} = V_1 = \frac{N_R * 100}{N_T} \quad (7)$$

$$\text{Oil percentage} = V_2 = \frac{N_B * 100}{N_T} \quad (8)$$

$$\text{Air percentage} = V_3 = \frac{N_{DB} * 100}{N_T} \quad (9)$$

Fig 4 shows an ECT image having 122 red pixels, 521 light blue pixels and 446 dark blue pixels. This information is used to calculate percentages of water, oil and air using the number of pixels for each of these materials and the total number of pixels of the image (Image analysis). For these pixel values, the percentages are 11.20 % for water, 47.84 % for oil and 40.96 % for air (Fig 4). These percentages of water, oil and air are stored in the knowledge base. After storing percentages of the components involved, the PCA part of the hybrid strategy completes.

The next stage is based on cluster analysis by which images are grouped together based on their similarities and differences. When an image of the process is generated (unknown image of process condition) then the two steps associated with CA are applied. In first step the Euclidean distance using 10 is evaluated to find the similar known images (in knowledge base) of this unknown image. This step is referred to as object recognition.

$$|M_1 - V_1| + |M_2 - V_2| + |M_3 - V_3| + |M_4 - V_4| + \dots + |M_z - V_z| \quad (10)$$

In above equation, V_1, V_2, \dots, V_z are the stored percentages of water, oil and air of the known images in the knowledge-base and $M_1, M_2, M_3, \dots, M_z$ are the calculated percentages for water, oil and air from the current unknown ECT image based on pixel information.

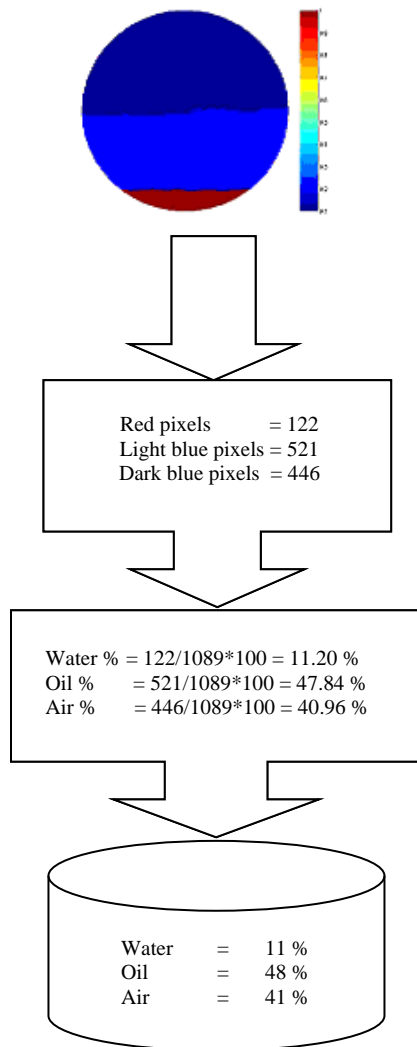


Fig 4 Image interpretation of experimental image

The knowledge base is searched to find the index i_1 of the closest match between unknown image and the stored known image. This index value is stored and compared with the index value i_2 of the image generated from ECT sensor at point 2 until they both come in a predefined limit (in this study it is $|i_1 - i_2| \leq 5$).

As soon as the values of both indices and Euclidean distances come within the range of ± 5 then it is concluded that the same process situation has reached from Sensor 1 to Sensor 2. The velocity profile is then calculated by using the distance between the two sensors and the amount of time involved in reaching the same process situation from Sensor 1 to Sensor 2.

For the calculation of volumetric flow rate, the average velocity and the area of cross section of the pipe are used. The volumetric flow rate is calculated as below:

$$\dot{V} = V_{avg} A \quad (11)$$

Where “ \dot{V} ” is the volumetric flow rate, “ V_{avg} ” is average velocity and “ A ” is the area of the cross section. The mass flow rate is then calculated by using following equation.

$$\dot{m} = \rho \dot{V} \quad (12)$$

In the above expression, “ \dot{m} ” is the mass flow rate and “ ρ ” is the density of the fluid in the pipeline. This expression can also be written as:

$$\dot{m} = \rho V_{avg} A \quad (13)$$

V_{avg} is calculated by dividing the distance between the two sensors with the time taken to reach the process condition from Sensor 1 to Sensor 2. To verify the propagation of a specific condition has reached from Sensor 1 to Sensor 2, the index values of the knowledge base are used.

Fig 6 shows images obtained from sensor 1 and sensor 2 having index difference $|i_1 - i_2| \leq 5$. By using above images the velocity comes out to be 4.5m/sec since sensor 1 and sensor 2 are placed at a distance of 2 metres. In this work 12 inch diameter piping is used so the area of cross section is 113.1 square inches (0.072 square metres).

The volumetric flow rate using 11 is given as below:

$$\dot{V} = V_{avg} A = 4.5 \times 0.072 = 0.324 \text{ m}^3/\text{sec}.$$

In this experiment, the sample of oil used has a density of 888.1 kg/m³ at room temperature, therefore the mass flow rate by 13 is given as

$$\dot{m} = \rho \dot{V} = 888.1 \times 0.32 = 287.74 \text{ kg/sec} = 4560.75 \text{ gal/min}$$

As mentioned in the literature, the typical mass flow rate through 12 inch diameter pipeline is about 4700 gal/min but it can vary depending upon type of oil, density, material of pipe,

pressure etc. It is expected that there will be an error of less than 5% as observed during experiments. This error value is acceptable for the flow estimations in the oil and gas industry.

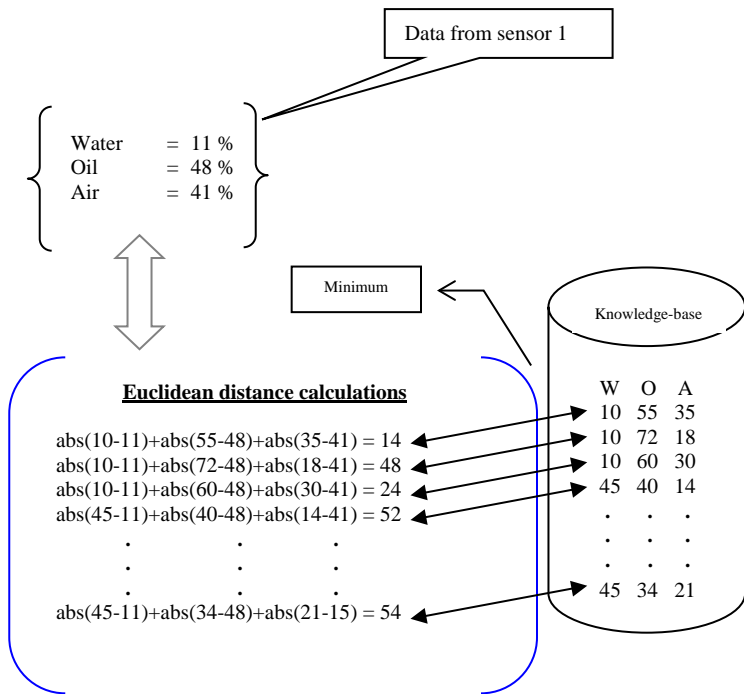


Fig 5 Steps during category recognition

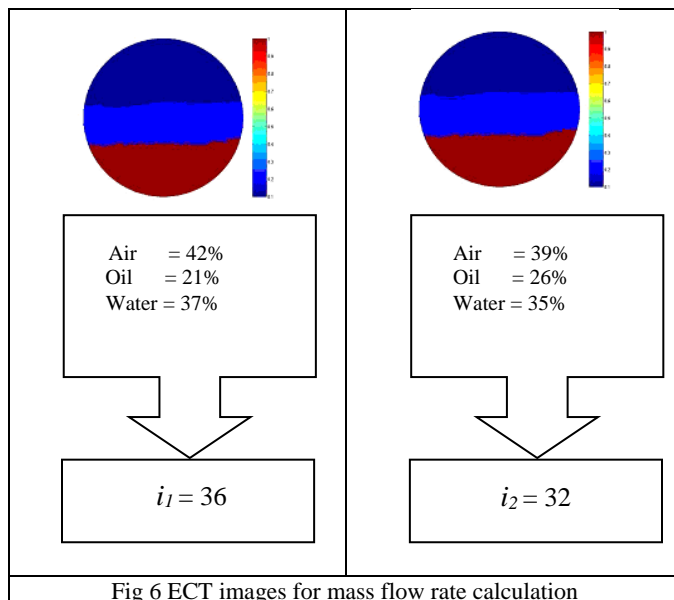


Fig 6 ECT images for mass flow rate calculation

This research leads to the following conclusions:

- A new hybrid approach has been developed by coupling ECT images with advanced statistics that can be used to design a novel multiphase flowmeter.
- It is envisaged that the proposed device will provide fast, accurate and reliable measurements and provide additional information on flow patterns and flow velocity typically not available with standard flow meters.
- Based on this work, the measurement accuracy and reliability can be further improved if three or more sensors are used at different locations.

ACKNOWLEDGMENT

S. F. A. Bukhari would like to take this opportunity to thank Cara (the Council for At-Risk Academics) for supporting this research at Brunel University London.

REFERENCES

- [1] A. Hijazi, A. Friedl, C. Cierpka, C. Kähler, and V. Madhavan, "High-speed imaging using 3CCD camera and multi-color LED flashes.", *Meas. Sci. and Technol.*, **11**(28), 2017.
- [2] R. Thorn, G. A. Johansen, and E. A. Hammer, "Three-phase flow measurement in the offshore oil industry, is there a place for process tomography?", *Proceedings of the 1st World Congress on Industrial Process Tomography*, 1999.
- [3] R. Thorn, G. A. Johansen, and B. T. Hjertaker, "Three phase flow measurement in the petroleum industry.", *Meas. Sci. and Technol.*, **24**, 2012.
- [4] M. Mao, J. Ye, H. Wang, and W. Q. Yang, "Investigation of gas-solids flow in a circulating fluidized bed using 3D electrical capacitance tomography.", *Meas. Sci. and Technol*, **27**(9), 2016.
- [5] Rocsole, <https://www.rocsole.com/products/applications/flow-watch>, Accessed on: 25 Feb. 2019.
- [6] G. Falcone, G. F. Hewitt, and C. Alimonti, "Multiphase flow metering.", Vol. 54, Elsevier Publication, 2012.
- [7] C. J. Werth, C. Y. Zhang, M. Brusseau, M. Oostrom, and T. Baumann, "A review of non-invasive imaging methods and applications in contaminant hydrogeology research", *Journal of Contaminated Hydrology*. **113**(1-4), pp. 1-24, 2013.

IV. CONCLUSION

- [8] R. Maad, G. A. Johansen, "Experimental analysis of high-speed gamma-ray tomography performance", *Meas. Sci. and Technol.*, 19(8), pp. 1-10, 2008
- [9] P. Mojabi, M. Ostadrahimi, L. Shafai, and J. LoVetri, "Microwave tomography techniques and algorithms: A review.", *Proceedings of 15th International Symposium on Antenna Technology and Applied Electromagnetics (ANTEM)*, 2012.
- [10] W. Q. Yang, M. S. Beck, and M. Byars, "Electrical capacitance tomography -- from design to applications." *Measurement + Control*, **28**, pp. 261-266, 1995.
- [11] W. Q. Yang, and M. Byars, "An improved normalisation approach for capacitance tomography", *Proc. of 1st World Congress on Industrial Process Tomography*, pp. 215-218, 1999.
- [12] C. Gamio, J. Castro, F. Garcia-Nocetti, L. Aguilar, L. Rivera, and H. Balleza, "High pressure gas-oil two-phase flow visualisation using electrical capacitance tomography.", *Proc. of 7th Biennial ASME Conference on Engineering Systems Design and Analysis ESDA 2004*, pp. 1-5, 2004.
- [13] T. Loser, R. Wajman, and D. Mewes, "Electrical capacitance tomography: image reconstruction along electrical field lines", *Meas. Sci. and Technol.*, **12**, pp. 1-9, 2001.
- [14] W. Q. Yang, and L. Peng, "Image reconstruction algorithms for electrical capacitance tomography.", *Meas. Sci. and Technol.*, **14**, pp. R1-R13, 2003.
- [15] J., Yao, and M. Takei, "Application of process tomography to multiphase flow measurement in industrial and biomedical fields - a review", *IEEE Sensors Journal*, 17(24), pp. 8196-8205, 2017.
- [16] X. Zhu, P. Dong, Q. Tu, Z. Zhu, W. Yang, and H. Wang, "Investigation of gas-solid flow characteristics in the cyclone dipleg of a pressurised circulating fluidised bed by ECT measurement and CPFD simulation.", *Meas. Sci. and Technol.*, **30**, 2019.